Impact of time interval alignment on data quality in electricity grids

Schwefel, Hans-Peter; Antonios, Imad; Lipsky, Lester

Published in:
2018 IEEE International Conference on Communications, Control, and Computing Technologies for Smart Grids (SmartGridComm)

DOI (link to publication from Publisher):
10.1109/SmartGridComm.2018.8587570

Publication date:
2018

Document Version
Early version, also known as pre-print

Impact of time interval alignment on data quality in electricity grids

Hans-Peter Schwefel
GridData GmbH
Anger, Germany
& Aalborg Univ.
schwefel@griddata.eu

Imad Antonios
Computer Science Department
Southern Connecticut State University
New Haven, CT, USA
antonios@southernct.edu

Lester Lipsky
Computer Science and Engineering
University of Connecticut
Storrs, CT, USA
lester.lipsky@uconn.edu

***Abstract*—Measurements of parameters in electricity grids are frequently average values over some time interval. In scenarios of distributed measurements such as in distribution grids, offsets of local clocks can result in the averaging interval being misaligned. This paper investigates the properties of the so-called time alignment error of such measurands that is caused by shifts of the averaging interval. A Markov model is derived that allows for numerically calculating the expected value and other distribution properties of this error. Actual consumption measurements of an office building are used to study the behavior of this time alignment error, and to compare the results from the trace with numerical results and simulations from a fitted Markov model. For increasing averaging interval offset, the time alignment error approaches a normal distribution, whose parameters can be calculated or approximated from the Markov model.**

***Index Terms*—Distribution Grid Measurements, Time Alignment Error, Data Quality, Markov Models.**

I. Introduction and Motivation

The amount of digital data sources in electricity distribution grids is rapidly increasing. Examples of measurement devices include smart meters and smart inverters at prosumer connection points or measurement devices in junction boxes and secondary substations. These devices typically provide values of voltages, currents, and power averaged over some logging interval of duration T, where T ranges from a few seconds to tens of minutes.

For some applications in energy grids such as the calculation of electricity losses in part of the grid, the data analytics software needs to correlate values from different measurement devices averaged over the *same* time interval $[t_i, t_i + T]$. As the measurement devices are geographically distributed, these time intervals may be subject to clock deviations. Typical clock deviation errors are in the order of few seconds [1], while they can be also larger in case of infrequent clock synchronization or slow and highly variable communication delays on the communication network between master clock and measurement devices. Any offset of the clock at the measurement device will in fact lead to a shifted averaging interval. Another cause of such shifted interval can result when there is no synchronization of clocks and the start of the averaging interval is determined by a request message from a data concentrator; the offset of the averaging interval is then determined by the selection of the request trigger at the concentrator and by the sum of the one-way communication delays and the required processing times of this request.

This paper provides an analysis of the impact of such offset, subsequently called δ, of the measurement interval on the value of the measured average. It thereby projects a timing error into the value domain of the measurand, making it possible to obtain confidence intervals for the measurand or other indicators of data quality. The paper then studies this error caused by the interval misalignment for changing sizes of the averaging interval T and for changing clock offset δ. Results shows that the error can for certain parameter ranges be approximated by a normal distribution, whose expected value can be calculated and standard deviation be approximated by a proposed mathematical model.

The quantification of the impact of measurement errors in different application contexts in general distributed systems has received increasing attention in the last few years. As one example of relevant research, measurement errors at the sensor may propagate through the whole computation chain, see, e.g., [5] for work characterizing such errors and their impact. Specifically in energy grids, recent work has addressed how to handle heterogeneous and noisy measurements in the context of grid estimation [3], [6], [10], [12]. Those papers focus mainly on noise on the measurands and how to include such noise characterization in grid estimation procedures. In contrast to that, this paper addresses the impact of time alignment errors for measurands that are averaged over a time interval.

The impact of timing in access to measurement information in distributed systems has earlier been analyzed in [4] and such analysis put into context of

different electricity grid applications in [7], [8] and also in generalized networked control applications [11]. This paper instead focuses on the deviations of a measurand caused by time alignment deviations at the sensor. The authors in [2] present an initial analysis of this aspect of the problem, however, their focus was on an empiric evaluation of the distribution of subsequent samples in a smart meter measurement trace. In contrast, this paper makes a detailed analysis of the impact of different interval offsets on measurement of averages using trace analysis, simulations, and a stochastic model.

In this paper we examine three views of electricity grids. One is a real measurement trace from a particular electrical grid. This trace is "exactly correct", but only for the four hours it measured. It tells us little about any other four hour period, and even less about other grids. A parameter-rich model must be made that in some sense represents the data. We have created a linear algebraic Markov model for that purpose, see [9] for theoretical details. The numerical results from evaluating the algebraic equations are very good for supplying parameter dependent expected values and also part of the distribution probabilities; furthermore, approximations of the standard deviation of the time alignment errors can be derived. The same model can be used in a Monte Carlo simulation. If the model is good, a particular trace will be probabilistically similar to the original measured trace and one can then generate many traces, whose average converges to the numerical results.

Section II formally introduces the time alignment error, ϵ, caused by the timing offset. Section III introduces a Markov-modulated model for the true measurand and shows examples of errors caused by time offset from a simulation of such models. Section IV derives expected values and other properties of the distribution of ϵ in the scenario of the Markov-modulated value process. Section V uses a measurement of power values at a customer connection point, fits a Markov-modulated process and studies the behavior of the time alignment error via numerical results from the Markov model and compares to trace-driven simulations.

II. System Description

In this paper, we focus on a single measurement device that determines values of a measurand m; here we assume that the physical measurand has the true behavior $m(t)$ and the measurement device determines the average value $\hat{m}(T,\delta)$ of $m(t)$ over a time interval $I = [\delta, \delta + T]$. Example scenarios are measurements of average voltage or average power in an electricity grid.

Our goal is to study the error of this measured average value that results from the shift of the measurement interval by some offset δ. Without loss of generality, we position the time interval of interest to start at $t = 0$. We then define the time averaged value of the measurand starting over a shifted interval with offset δ:

$$\hat{m}(T,\delta) := 1/T \int_{\delta}^{T+\delta} m(t)dt. \quad (1)$$

The desired value is for $\delta = 0$, but the offset $\delta > 0$ can be caused by different reasons including non-ideal clock synchronization. Therefore, it is of interest to examine their difference. In order to achieve this, this paper derives and presents results on the behavior of the random variable

$$\epsilon(T,\delta) := \hat{m}(T,0) - \hat{m}(T,\delta), \quad (2)$$

for different stochastic processes $m(t)$ and different choices of $T \in \mathrm{R}^+$ and $\delta \in \mathrm{R}$. We call ϵ the resulting interval alignment error caused by an interval offset of δ and for an averaging period of duration T.

III. Markov model

We model the behavior of $m(t)$ by a Markov chain model with generator matrix $\mathbf{Q}$. The state of the Markov chain model, $S(t) = i$, at time t determines the value of physical measurand $m(t) = \nu_i$. While ν_i can represent any type of measurement, we explain and apply the model in this paper in the context of power measurements, so $m(t)$ is the consumed (or, with a different sign, produced) power at a grid connection, as e.g. measured by a smart meter.

We assume that the measurement is taken at a prosumer with n discrete levels of power and hence $\dim\mathbf{Q} = n$. The time that the Markov chain spends in level j is exponentially distributed, with mean time $1/\mu_j = 1/Q_{jj}$, where $1 \leq j \leq n$. [Note that we use the convention in [9], which is the negative of other texts.] The power consumed or injected when at that level is ν_j.

For future reference, we also define the (diagonal) power consumption matrix,

$$[\mathbf{E}]_{jj} = \nu_j.$$

There exists a steady-state $\boldsymbol{\pi}$ satisfying $\boldsymbol{\pi}\mathbf{Q} = \mathbf{0}$ which can be normalized so that $\boldsymbol{\pi}\boldsymbol{\varepsilon}' = 1$.

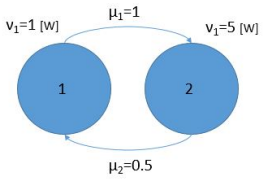

Fig. 1: Example of 2-state Markov chain representation.

In order to illustrate the Markov model, we now present and discuss simulation results for the distribution

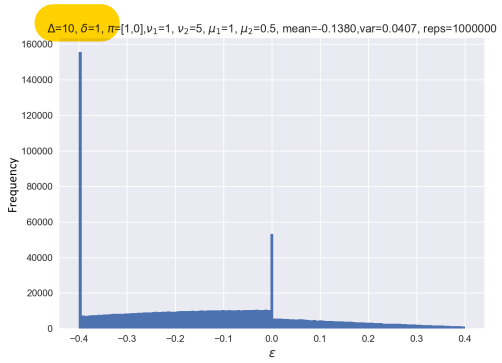

Fig. 2: Simulation of two-state model: $\pi(0) = [1, 0]$

of $\epsilon(T, \delta) := \hat{m}(T, 0) - \hat{m}(T, \delta)$ for the simplest model of a 2-state Markov process shown in Figure 1.

Figures 2 shows the resulting distribution of ϵ from simulations of the same 2-state Markov model, where the Markov process at the beginning of the measurement interval starts in state 1. The figure shows that the value of ϵ is bounded; the distribution shows discrete spikes at 0 and at the minimum, with continuous density in between. More discussion on this property will follow in the next section.

IV. Numerical Calculation of Time Alignment Errors

This section uses the Markov model for the true behavior of the physical measurand, here always assumed to be power, in order to derive equations for the calculation of different properties of the averaged measurand $\hat{m}(T, \delta)$ and of the time alignment error $\epsilon(T, \delta)$.

A. Expected values

One form of the Chapman-Kolmogorov equation states that

$$\frac{d\boldsymbol{\pi}(t)}{dt} = -\boldsymbol{\pi}(t)\mathbf{Q},$$

which has the solution

$$\boldsymbol{\pi}(t) = \boldsymbol{\pi}(0)\mathbf{G}(t) := \boldsymbol{\pi}(0)\exp(-t\mathbf{Q}). \tag{3}$$

$[\boldsymbol{\pi}(t)]_j$ is the probability that the system will be in state j at time t, but we would like to know how long the system spent in state j during a given time interval, T. This is simply the system vector:

$$\boldsymbol{\tau}(T) = \int_0^T \boldsymbol{\pi}(t)\,dt$$

$$= \boldsymbol{\pi}(0)\int_0^T \mathbf{G}(t)\,dt =: \boldsymbol{\pi}(0)\mathbf{H}(T).$$

That is, $[\boldsymbol{\tau}(T)]_j$ is the total time the system spent in state j in the time interval T. Observe that since $\mathbf{Q}\boldsymbol{\varepsilon}' = 0$, it follows that $\mathbf{G}(\mathbf{t})\boldsymbol{\varepsilon}' = \boldsymbol{\varepsilon}'$. Therefore $\mathbf{H}(T)\boldsymbol{\varepsilon}' = T\boldsymbol{\varepsilon}'$, and thus

$$\boldsymbol{\tau}(T)\boldsymbol{\varepsilon}' = T.$$

The problem is, the integral cannot be carried out formally, because $\mathbf{Q}$ has no inverse. Instead we must replace it by its *spectral decomposition*. More precisely we replace $\exp(-t\mathbf{Q})$. That is,

$$\mathbf{G}(t) = \exp(-t\mathbf{Q}) = \boldsymbol{\varepsilon}'\boldsymbol{\pi} + \sum_{j'}^{n} e^{-t\lambda_j}\mathbf{v}'_\mathbf{j}\,\mathbf{u}_\mathbf{j}, \tag{4}$$

where λ_j is a non-zero eigenvalue of $\mathbf{Q}$, and $\mathbf{v}'_\mathbf{j}$, and $\mathbf{u}_\mathbf{j}$ are its right- and left-eigenvectors. The "$'$" with j tells us that the sum excludes the eigenvalue, $\lambda_j = 0$.

Putting this into the integral yields

$$\mathbf{H}(T) := \int_0^T \mathbf{G}(t)\,dt$$

$$= \boldsymbol{\varepsilon}'\boldsymbol{\pi}T + \sum_{j'}^{n} \frac{1}{\lambda_j}[1 - e^{-T\lambda_j}]\mathbf{v}'_\mathbf{j}, \mathbf{u}_\mathbf{j}. \tag{5}$$

Note that

$$\lim_{T\to\infty} \frac{\mathbf{H}(T)}{T} = \boldsymbol{\varepsilon}'\boldsymbol{\pi}.$$

In other words, if the measuring interval T is large enough, the steady-state solution is seen, no matter what the initial state was. The approach to its limit goes as $\mathrm{O}(1/T)$, which could mean that T has to be pretty big.

Another relation between $\mathbf{G}$ and $\mathbf{H}$ can be found by observing that

$$\mathbf{Q}\,\mathbf{H}(T) = \int_0^T \mathbf{Q}\,\mathbf{G}(t)\,dt = \mathbf{I} - \mathbf{G}(T). \tag{6}$$

This will be useful below.

Next we have to calculate the expected value of the average power in that time period:

$$\mathbb{E}[\hat{m}(T, 0)] := \frac{1}{T}\boldsymbol{\tau}(T)\mathbf{E}\boldsymbol{\varepsilon}' = \frac{1}{T}\boldsymbol{\pi}(0)\mathbf{H}(T)\mathbf{E}\boldsymbol{\varepsilon}'. \tag{7}$$

Note that the j^{th} component of the column vector, $\mathbf{H}(T)\mathbf{E}\boldsymbol{\varepsilon}'$, is the expected value of the average power in the interval, T, when starting in state j, so we get them all in one shot!

Figure 3 shows the numerical results for the behavior of the average power for the two-state Markov chain example. The figure shows the value of $\mathbb{E}[\hat{m}(T, \delta)]$ for two initial conditions and three values of $\delta = 0, 1, 2$. All six curves are approaching the steady-state value of $\boldsymbol{\pi}\mathbf{E}\boldsymbol{\varepsilon}'' = 3.6667$.

The next question to answer is "What if measurement began a small time, δ, later? What would the expected value of the average power for the period be?" From (3) we get the state of the system at time δ, namely,

$$\boldsymbol{\pi}(\delta) = \boldsymbol{\pi}(0)\mathbf{G}(\delta).$$

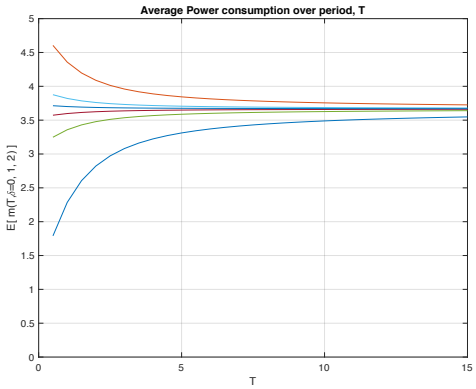

Fig. 3: Average power for 2-state model in Figure 1 as a function of T for different initial state power levels. The lowest three curves are for $\boldsymbol{\pi}(0) = [1\ 0]$. The innermost pair are for $\delta = 2$.

Then

$$\mathbb{E}[\hat{m}(T,\delta)] = \frac{1}{T}\boldsymbol{\pi}(\delta)\mathbf{H}(T)\mathbf{E}\boldsymbol{\varepsilon}'$$

$$= \frac{1}{T}\boldsymbol{\pi}(0)\mathbf{G}(\delta)\,\mathbf{H}(T)\mathbf{E}\boldsymbol{\varepsilon}'. \tag{8}$$

The expected change in $\mathbb{E}[\hat{m}]$ with change of offset is:

$$\mathbb{E}[\epsilon(T,\delta)] := \mathbb{E}[\hat{m}(T,0)] - \mathbb{E}[\hat{m}(T,\delta)]$$

$$= \frac{1}{T}\boldsymbol{\pi}(0)\,[\mathbf{I} - \mathbf{G}(\delta)]\,\mathbf{H}(T)\mathbf{E}\boldsymbol{\varepsilon}'. \tag{9}$$

With the aid of (6) this can also be written as

$$\mathbb{E}[\epsilon(T,\delta)] = \frac{1}{T}\boldsymbol{\pi}(0)\mathbf{Q}\,\mathbf{H}(\delta)\mathbf{H}(T)\mathbf{E}\boldsymbol{\varepsilon}'. \tag{10}$$

Note that since $\boldsymbol{\pi}\,\mathbf{Q} = \mathbf{0}$, the last equation shows that $\mathbb{E}[\epsilon(T,\delta)] = 0$ when the Markov process is in its steady state at the beginning of the measurement interval. Therefore, the time alignment error will in this case be an unbiased error.

B. Approximation of standard deviation of the alignment error distribution

The mean power consumption as a function of time can be very dependent on the initial conditions if the measured time period is not too long, (see Figure 3). Similarly, the expected values of ϵ also vary with different initial states. By removing $\boldsymbol{\pi}(0)$ from Eq. 9 we get:

$$\mathbb{E}[\epsilon_j(T,\delta)] := \frac{1}{T}[[\mathbf{I} - \mathbf{G}(\delta)]\,\mathbf{H}(T)\mathbf{E}\boldsymbol{\varepsilon}']_j.$$

If the initial condition is not known we can assume steady state conditions. The variance of ϵ can then be approximated by the variability of the $\mathbb{E}[\epsilon_j]$ as follows: (note that the expected value of ϵ is zero in steady state initial condition):

$$\sigma_s^2 := \mathrm{Var}(\epsilon) \approx \sum_{i=0}^{n} \pi_i \cdot \mathbb{E}[(\epsilon_i)]^2.$$

C. Calculation of discrete probabilities of error distribution

The earlier simulation results for a 2-state Markov chain show discrete probabilities at three values of ϵ. We now explain the reason of these discrete components and present equations for the resulting probabilities.

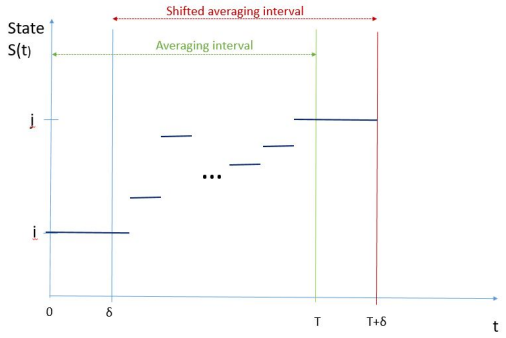

Fig. 4: Scenario causing discrete probabilities in the mixed discrete continuous distribution of ϵ for a Markov modulated value process

Figure 4 shows a scenario which has a discrete occurrence probability:

- The Markov process is in State i at time $t = 0$ with probability and remains in State i for at least the duration of δ. The probability of this first condition to be true is:

$$p_i = [\boldsymbol{\pi}(0)]_i \cdot e^{-\mu_i \delta}. \tag{11}$$

- At the end of the original averaging interval at time T, the Markov process is in state j and remains there for a time period of at least duration δ. The probability of the latter occurring is:

$$p_j = [\exp[-\mathbf{Q}(T-\delta)]]_{ij} e^{-\mu_j \delta}$$

$$= [\mathbf{G}(T-\delta)]_{ij} e^{-\mu_j \delta} \tag{12}$$

Putting these two equations together, the probability of having this case occur is:

$$p_{ij} := [\boldsymbol{\pi}(0)]_i \cdot e^{-\mu_i \delta} \cdot [\mathbf{G}(T-\delta)]_{ij} \cdot e^{-\mu_j \delta}. \tag{13}$$

The corresponding value of the resulting alignment error that occurs with the probability as stated above is:

$$\epsilon(T, \delta \,|\, i, j) := \frac{\nu_i \cdot \delta - \nu_j \cdot \delta}{T}. \tag{14}$$

V. Case Study: Application to power measurement data

We now investigate the measurement error ϵ in an actual power measurement trace. As it is practically infeasible to have continuous measurements of $m(t)$, typically all traces already represent average values over some time interval. We therefore utilized traces with small measurement interval of $1s$ in order to allow suitable evaluation of ϵ when δ and T vary over ranges of several seconds to few minutes.

A. Power Measurement Data

In order to apply the model and analysis of the distribution of ϵ to some real power measurements, we used a measurement trace of a grid connection point that connects a medium-sized office building. Part of the behavior of the measured power in 1 second intervals is shown in Figure 5. The average power is 8.137 kW when considering the full measurement of about 9650 samples.

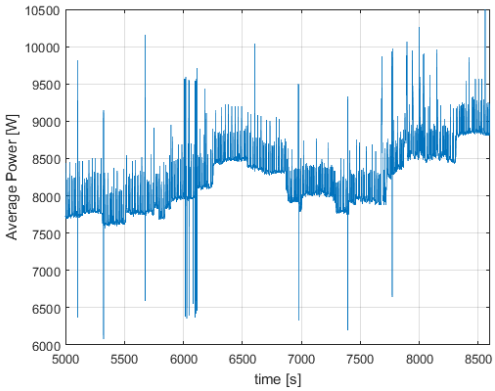

Fig. 5: Measurements of energy in 1-sec intervals at connection of medium-sized office building

The corresponding histogram of the 1s power values is shown in Fig. 6. Based on the spikes of the histogram, we fitted a Markov chain with 12 states to this data: the dashed lines in the figure mark the discretization boundaries; the corresponding levels ν_i for state i were determined by the mean of the values between boundary i and $i+1$.

We use the resulting Markov model and the true measured trace subsequently to show properties of the measurement error caused by clock offset. Figure 7 shows the histogram of the error ϵ as resulting in the trace when using an averaging window of size $T = 100s$ and a clock offset of $\delta = 8s$. The histogram has been obtained by sliding the averaging interval over the measurement data. The resulting mean error $\mathbb{E}(\epsilon) \approx 0.4165W$ is small but the standard deviation $\text{std}(\epsilon) \approx 20.6W$, or relative to the mean value of the measurand, about $2.5 \cdot 10^{-3}$. Note that this relative error is in the same order of magnitude of

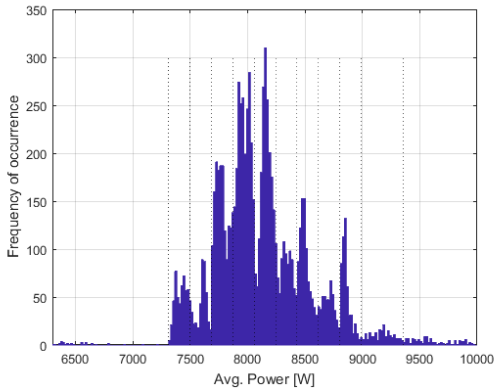

Fig. 6: Histogram of the energy measurements and visualization of the boundaries for discretization in Markov model

what is typically seen as measurement noise in practical smart meter deployments [], so it should be taken into account.

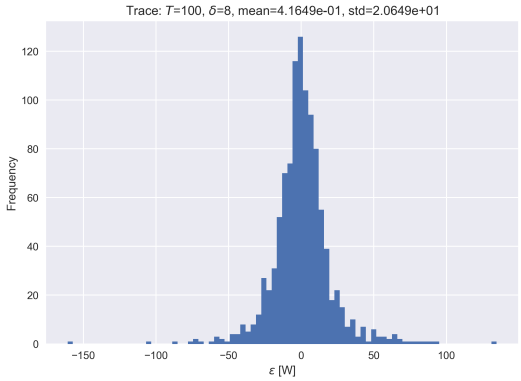

Fig. 7: Histogram of ϵ as resulting from the measurement trace using a sliding time interval of duration $T = 100s$ and an interval offset of $\delta = 8s$.

B. Simulation results for fitted Markov model

The fitted Markov model is now used in simulations to investigate the behavior of the distribution of ϵ considering steady-state as initial condition. Steady-state is a concept from probability theory, and it takes some effort to apply it to actual traces and Monte Carlo simulations. After all, a system can only be in one state at a time, whereas the $i-th$ component of π is the *probability* that the system is in state i. In simulations, the simulation is run many times with the starting state i occurring according to π_i.

Figure 8 shows the alignment error distribution from simulations of the fitted Markov model started according to the steady-state probabilities at $t = 0$ and for

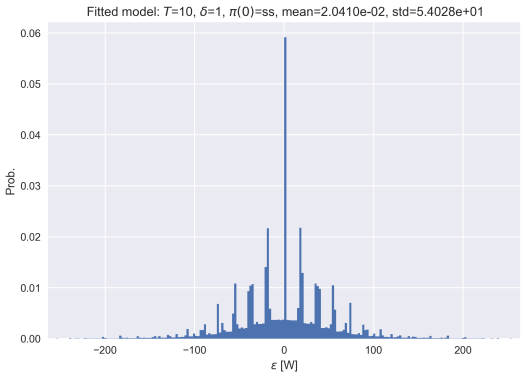

Fig. 8: Histogram of ϵ for the fitted Markov model using simulations with $T = 10s$, $\delta = 1s$ and starting with steady-state probabilities.

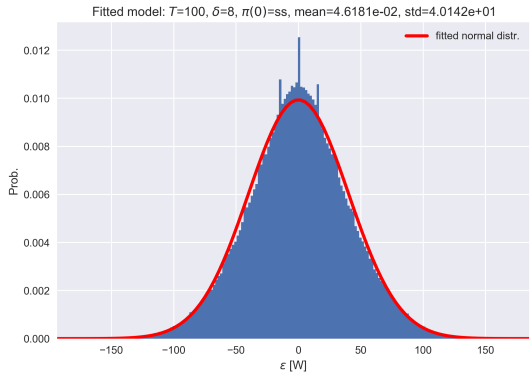

Fig. 9: Histogram of ϵ for the fitted Markov model using simulations with $T = 100s$, $\delta = 8s$ and starting with steady-state probabilities. The overlaid smooth curve is that of a normal distribution with matching mean and standard deviation.

averaging interval size of $T = 10$s and offset $\delta = 1$s. The resulting distribution is symmetric, has mean close to 0 (as the analytic results in Equation (10) showed) and shows a number of spikes due to the discrete probabilities, see Equation 13 with $i, j = 1...12$. When simulating the same case for different T, the resulting distribution is just scaled on the x-axis with $1/T$, not shown here due to space limitations.

The spikes in the previous histograms are a consequence of the discrete probabilities in the distribution of ϵ and their size reduces with increasing value of δ, see the calculations in Section IV-C. When increasing δ, the distribution of ϵ becomes close to a normal distribution, as shown in Figure 9 ($\delta = 8$) and even more for Figure 10. The case of normally distributed alignment error is interesting as it can be easily combined with other normally distributed errors such as the measurement error. A QQ plot and normality tests, not shown here, confirm the fit to a normal distribution, when $\delta > 10s$ approximately.

Finally, the simulation estimate for mean and standard deviation of ϵ when using the fitted Markov model is compared with an estimate directly from the trace in Figure 11. Note that the plotted standard deviation in the figure is scaled by $1/\sqrt{\delta}$ to show its convergence. As a consequence of the scaling, the unscaled actual standard deviations grow more strongly as opposed to the scaled version shown in the figure. Note that the full measurement trace contains about 9650 observations, which results in a sample size of $(9650 - T - \delta)/\delta$ from the sliding window calculation of ϵ, so the number of samples for the mean and standard deviation estimation for the trace (blue curves in Fig. 11) reduces for increasing T and deviations from the expected $\mathbb{E}[\epsilon] = 0$ value occur for large T due to the lack of samples.

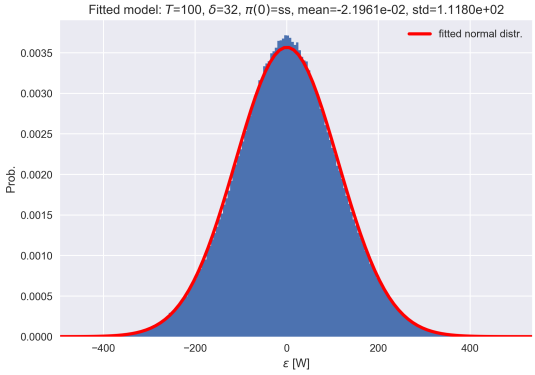

Fig. 10: Same as Figure 9, but with $\delta = 32s$.

Note that the simulation of the Markov model leads to a substantially larger standard deviation estimate $std(\epsilon)$; this may be due to the discretization of the power measurements in twelve discrete values.

C. Comparison with analytic model

Finally, we compare the analytic calculations of the expected value of ϵ and the approximation of its variance to both a simulation and the data. Figure 12 shows this comparison, now for increasing T. Note that the increase of T does not have the same strong impact on number of samples contributing to epsilon estimates from the trace as in the previous figure (that varied δ). Hence, the mean estimate of ϵ from the trace stays close to the analytic results, which is exactly on zero. The standard deviation of ϵ reduces as $1/T$, so the variability of the time alignment error reduces with the same decay in both the simulation and the trace-based analysis. The standard

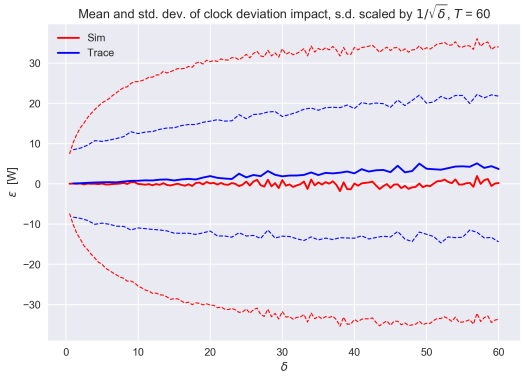

Fig. 11: Behavior of the mean and the scaled standard deviation of the alignment error for fixed interval size $T = 60s$ and increasing offset δ comparing the measurement trace and simulation with the steady state as the initial condition.

estimation from the simulation in Figure 12 is almost exactly a factor 2 larger than the analytic approximation. The standard deviation estimate from the trace, however, is suprisingly close to the analytic approximation. This observation will be investigated further in future work.

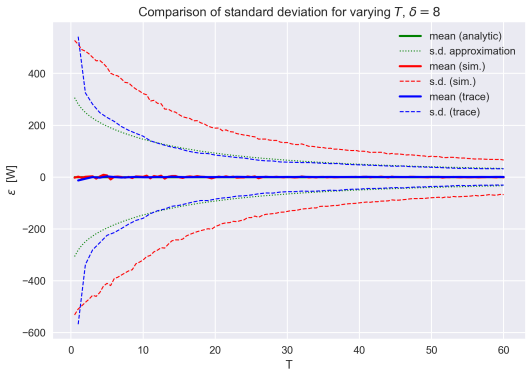

Fig. 12: Comparison of standard deviation of ϵ.

VI. Conclusions

This paper defines and analyzes the time alignment error caused by offsets of the averaging interval for measurements in distribution grids. The time alignment error is formally defined and its behavior is investigated for an actual high-resolution power measurement trace, for the simulation of a Markov-modulated process that is fitted to the measurement data, and via matrix-algebraic calculations on the same Markov process. The results show that the time alignment error approaches a normal distribution for increasing offset δ. The mathematical model can be used to determine parameters of the normal distribution, so that this measurement error can be used in further processing of the data.

Future analysis will investigate the impact of parameters for the Markov model fitting on the time alignment error distribution; furthermore, the application of the model and of the analysis can be applied to other measurements than power, e.g. to average voltages in distribution grids. A more detailed investigation of the nearly constant factor between variance approximation from the analytic model and observed variance estimate for ϵ from the data should also be performed.

Acknowledgment

This work was supported by the European Unions Horizon 2020 research and innovation program under grant agreement No 774145 within the project Net2DG. The authors would like to thank all project partners for their feedback and input. In particular, the authors would like to thank Robert Damboeck, Stadtwerke Landau a.d. Isar for providing access to the measurement data in Section V.

References

[1] European norm 50470: Electricity metering equipment (a.c.), 2006.

[2] A. Alimardani, F. Therrien, D. Atanackovic, J. Jatskevich, and E. Vaahedi. Distribution system state estimation based on nonsynchronized smart meters. *IEEE Access*, 2017.

[3] S. Bhela, V. Kekatos, and S. Veeramachaneni. Enhancing observability in distribution grids using smart meter data. *IEEE Transactions on Smart Grid*, 2016.

[4] M. Bøgsted, R. L. Olsen, and H.-P. Schwefel. Probabilistic models for access strategies to dynamic information elements. *Performance Evaluation*, 67(1):43 – 60, 2010.

[5] T. Brade, S. Zug, and J. Kaiser. Validity-based failure algebra for distributed sensor systems. In *32nd International Symposium on Reliable Distributed Systems (SRDS)*, pages 143–152. IEEE, 2013.

[6] J.-C. Chen, H.-M. Chung, C.-K. Wen, W.-T. Li, and J.-H. Teng. State estimation in smart distribution system with low-precision measurements. *IEEE Transactions on Smart Grid*, 2015.

[7] T. M. J. Madsen, M. Findrik and H.-P. Schwefel. Optimizing data access for wind farm control over hierarchical communication networks. *International Journal of Distributed Sensor Networks*, 12(5), 2016.

[8] T. le Fevre Kristensen, R. L. Olsen, H.-P. Schwefel, and J. G. Rasmussen. Information access for event-driven smart grid controllers. *Sustainable Energy, Grids and Networks*, 13:78–92, March 2018.

[9] L. Lipsky. *Queueing Theory: A Linear Algebraic Approach*. Springer, 2nd edition, 2009.

[10] R. Masud. *Smart grid state estimation and its applications to grid stabilization*. PhD thesis, University of Technology Sydney, 2017.

[11] R. Olsen, J. T. Madsen, J. Rasmussen, and H.-P. Schwefel. On the use of information quality in stochastic networked control systems. *Computer Networks*, 124:157–169, Sept. 2017.

[12] H.-P. Schwefel, J. G. Rasmussen, R. L. Olsen, and H. Ringgaard. Characterization of data quality in low-voltage grid estimation. In *Submitted for Review*.